

An Efficient and Multi-Modal Navigation System with One-Step World Model

Wangtian Shen¹, Ziyang Meng^{1*}, Jinming Ma², Mingliang Zhou² and Diyun Xiang²

¹Tsinghua University, ²Xiaomi (China)

swt22@mails.tsinghua.edu.cn, ziyangmeng@tsinghua.edu.cn, majinming3@xiaomi.com, zhoumingliang@xiaomi.com, xiangdiyun@gmail.com

Abstract

Navigation is a fundamental capability for mobile robots. While the current trend is to use learning-based approaches to replace traditional geometry-based methods, existing end-to-end learning-based policies often struggle with 3D spatial reasoning and lack a comprehensive understanding of physical world dynamics. Integrating world models—which predict future observations conditioned on given actions—with iterative optimization planning offers a promising solution due to their capacity for imagination and flexibility. However, current navigation world models, typically built on pure transformer architectures, often rely on multi-step diffusion processes and autoregressive frame-by-frame generation. These mechanisms result in prohibitive computational latency, rendering real-time deployment impossible. To address this bottleneck, we propose a lightweight navigation world model that adopts a one-step generation paradigm and a 3D U-Net backbone equipped with efficient spatial-temporal attention. This design drastically reduces inference latency, enabling high-frequency control while achieving superior predictive performance. We also integrate this model into an optimization-based planning framework utilizing anchor-based initialization to handle multi-modal goal navigation tasks. Extensive closed-loop experiments in both simulation and real-world environments demonstrate our system’s superior efficiency and robustness compared to state-of-the-art baselines. Project page: <https://robotnav-bot.github.io/nav-onestepwm/>

1 Introduction

Visual navigation constitutes a cornerstone of autonomous robotics, enabling robots to perceive their surroundings and reach target goals in complex, unstructured environments. In recent years, by leveraging large-scale datasets, methods like GNM [Shah *et al.*, 2023a], ViNT [Shah *et al.*, 2023b] and No-MaD [Sridhar *et al.*, 2024] have demonstrated remarkable ro-

bustness and generalization capabilities. However, these end-to-end policies often operate as “black boxes”, mapping observations directly to actions without explicit 3D spatial reasoning, which limits their performance in challenging navigation tasks.

World models [Ha and Schmidhuber, 2018] offer a promising alternative to end-to-end policies by enabling robots to ‘imagine’ outcomes, thereby enhancing spatial reasoning [Yang *et al.*, 2025]. While recent works integrate video prediction with planning [Bar *et al.*, 2025; Zhou *et al.*, 2025], practical deployment faces a critical bottleneck: computational latency. State-of-the-art models predominantly rely on diffusion frameworks, where iterative denoising and autoregressive generation accumulate significant latency and errors. This overhead becomes prohibitive when coupled with planning algorithms that evaluate multiple action candidates, hindering real-time usage. Furthermore, while prior works primarily focus on open-loop, image-goal evaluations, navigation world models have the potential to handle multi-modal goals, and closed-loop experiments in both simulation and real-world environments are essential for validating their effectiveness.

In this work, we propose a lightweight navigation world model designed specifically for real-time inference. Unlike standard diffusion-based approaches that suffer from slow iterative sampling, our model adopts the one-step generation paradigm [Frans *et al.*, 2024]. This drastically reduces the inference time required to predict future observations, making it feasible to integrate predictive modeling into high-frequency control loops. Additionally, we introduce a computation-efficient spatial-temporal attention mechanism embedded within a 3D U-Net backbone, enabling the model to simultaneously predict all future frames in a non-autoregressive manner. This synergistic design substantially boosts generation efficiency while effectively enhancing the quality of the predicted sequences. To further improve performance in limited-data regimes, we incorporate strategic pre-training and random trajectory sampling to facilitate robust generation.

Building upon this efficient world model, we integrate it with an optimization-based planning framework, utilizing task-specific loss functions to iteratively refine action samples. Such an integration enables navigation under multi-modal goal conditions, successfully encompassing image-

*Corresponding author

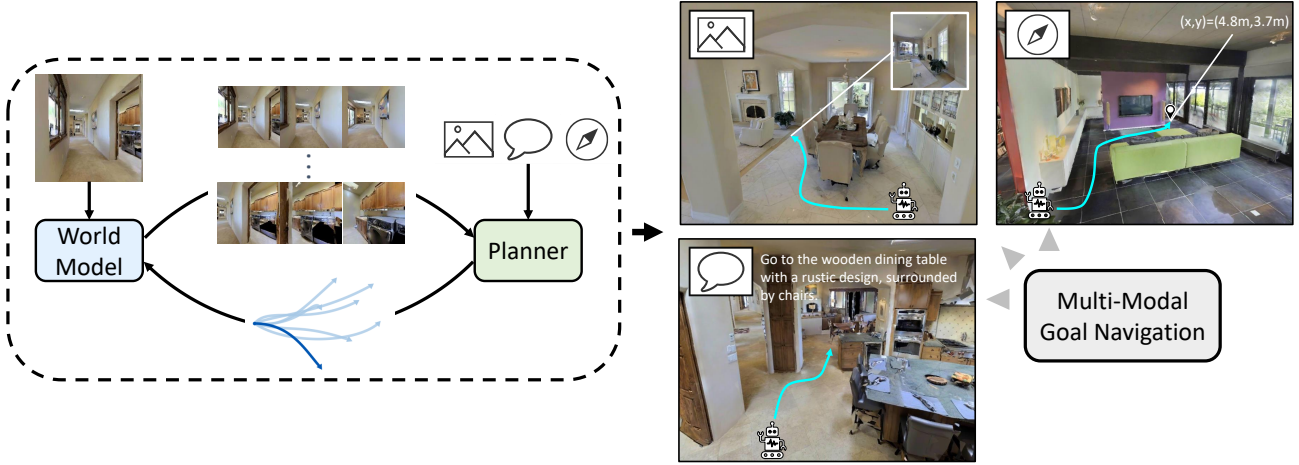


Figure 1: We present a unified navigation framework founded on world models and planning strategies. The proposed system can be directly used to support diverse goal modalities, seamlessly accommodating image-goal, language-goal, and point-goal navigation tasks.

goal, language-goal, and point-goal navigation tasks in a unified framework, as illustrated in Figure 1. Through a comprehensive exploration of trajectory initialization strategies and loss function designs, we establish a planning framework with superior performance. These efforts cumulatively produce a robust, closed-loop world-model-based navigation system, which we demonstrate to be both effective and efficient in simulation and real-world environments.

Our main contributions are summarized as follows:

- We propose a lightweight but effective navigation world model leveraging one-step generation paradigm, spatial-temporal attention, and pretraining strategy.
- We develop a unified navigation system for multi-modal goal navigation by integrating our world model with a planning framework utilizing anchor-based initialization.
- We demonstrate the superiority of the proposed method through closed-loop experiments in both simulation and the real world.

2 RELATED WORK

2.1 Learning Based Visual Navigation

Traditional solutions to navigation problem typically consist of distinct localization, mapping, and planning modules [LaValle, 2006]. The advent of machine learning shifts the focus towards learning-based solutions for visual navigation. GNM [Shah *et al.*, 2023a] shows that training on diverse robotic datasets boosts generalization. ViNT [Shah *et al.*, 2023b] and EffoNAV [Shen *et al.*, 2025] further advance this by employing transformer architectures and visual foundation models to establish foundational models for image-goal navigation in general environments. NoMaD [Sridhar *et al.*, 2024] leverages diffusion model to execute both navigation and exploration tasks within a single framework. NavDP [Cai *et al.*, 2025] enables robust and efficient sim-to-real navigation by leveraging diffusion-based trajectory generation alongside a

critic function. LeLaN [Hirose *et al.*, 2024] learns language-conditioned navigation policies from unlabeled and action-free videos. OmniVLA [Hirose *et al.*, 2025] presents a generalizable and flexible omni-modal robotic foundation model. Although significant progress has been made by introducing learning-based solutions for navigation, current methods exhibit limited spatial reasoning abilities, leading to suboptimal navigation performance.

2.2 World Model for Embodied Intelligence

Unlike end-to-end policy, the primary objective of a world model [Ha and Schmidhuber, 2018] is to simulate environmental dynamics. While early research focused on enhancing sample efficiency in reinforcement learning [Hafner *et al.*, 2019; Hafner *et al.*, 2023], recent works leverage world models for high-dimensional visual generation and planning. Approaches like Pathdreamer [Koh *et al.*, 2021], UniPi [Du *et al.*, 2023], and Genie [Bruce *et al.*, 2024] generate plausible future observations to facilitate interaction and navigation. Furthermore, integrating world models with planning has shown significant promise. NWM [Bar *et al.*, 2025] utilizes generative predictions to optimize action sequences, while [Zhou *et al.*, 2025] introduce 3D memory for temporal consistency. However, the high computational cost of these generative processes makes real-time deployment impossible. On the other hand, approaches like DINO-WM [Zhou *et al.*, 2024] and [Zhang *et al.*, 2025] construct world models within the latent space to minimize computational overhead. However, performing generation and planning solely in the latent space often cannot produce explicit 3D spatial prediction and different goal modals cannot be integrated into a unified framework.

3 METHODS

3.1 One-Step World Model for Navigation

Formally, the navigation world model is designed to predict the future observation $s_{\tau+1}$ based on the current observa-

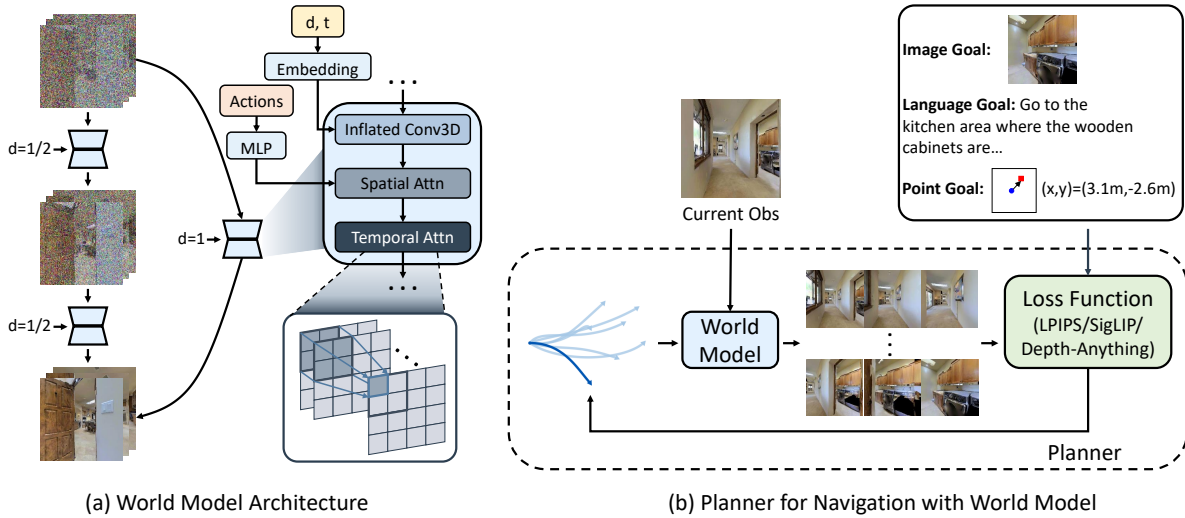


Figure 2: Illustration of our world model architecture and the world model-based planner. (a) Architecture of the proposed navigation world model. Built upon a 3D U-Net backbone, the model integrates convolutional layers with spatial-temporal attention blocks and is trained using a shortcut objective. (b) The action optimization process conditioned on navigation goals. Leveraging the world model, we utilize a loss function to score action candidates, thereby enabling navigation with multi-modal goals.

tion s_τ and the action a_τ . While existing generative approaches typically leverage diffusion models[Ho *et al.*, 2020; Song *et al.*, 2020] or flow-matching models[Lipman *et al.*, 2022], their sampling processes require iterative denoising over numerous neural network passes, rendering the generation computationally expensive. To address this issue, we adopt the shortcut training objective [Frans *et al.*, 2024] to enable one-step generation, thereby significantly reducing computational inference time. The shortcut model is conditioned not only on the flow timestep t , but also on a desirable step size d . Formally, the world model f_θ predicts the velocity vector $v_t = f_\theta(s_{\tau+1}^{(t)}, s_\tau, a_\tau, t, d)$, where $s_{\tau+1}^{(t)}$ represents the noisy future observation. For the minimum step size d_{\min} , the model is trained using the standard flow matching loss. For larger step sizes $d_{\min} < d < 1$, a bootstrap consistency loss that distills the trajectory of two smaller substeps (size $d/2$) into a single step is employed, as shown in Figure 2(a). The training objective is formulated as follows:

$$s_{\tau+1}^{(0)} \sim \mathcal{N}(0, I), \quad s_{\tau+1}^{(1)} \sim \mathcal{D}(\text{Dataset}), \quad (1)$$

$$\mathcal{L}(\theta) = \left\| f_\theta(s_{\tau+1}^{(t)}, s_\tau, a_\tau, t, d) - v_{\text{target}} \right\|^2, \quad (2)$$

$$v_{\text{target}} = \begin{cases} s_{\tau+1}^{(1)} - s_{\tau+1}^{(0)}, & \text{if } d = d_{\min}, \\ \frac{1}{2}(v' + v''), & \text{otherwise,} \end{cases} \quad (3)$$

$$\text{where } v' = f_\theta(s_{\tau+1}^{(t)}, s_\tau, a_\tau, t, d/2), \quad (4)$$

$$v'' = f_\theta(s_{\tau+1}^{(t)}, s_\tau, a_\tau, t + \frac{d}{2}, d/2), \quad (5)$$

$$s'_{\tau+1} = s_{\tau+1}^{(t)} + v' \cdot \frac{d}{2}. \quad (6)$$

By employing this distillation training, the navigation world model learns to generate future observations from gaussian

noise within one step.

3.2 Architecture of Navigation World Model

Following the formulation in the previous section, we now provide the implementation details of the world model f_θ . Existing navigation world models[Bar *et al.*, 2025] in navigation predominantly adopt an autoregressive approach, generating predictions iteratively frame-by-frame. We argue that such autoregressive methods suffer from performance degradation due to error accumulation over long horizons and result in high computational latency. Instead, the proposed architecture utilizes a 3D U-Net backbone to simultaneously predict a sequence of 11 future frames. Drawing inspiration from the Stable Diffusion framework [Rombach *et al.*, 2022], we employ a hybrid structure integrating both CNNs and transformers to capture spatiotemporal dependencies, as illustrated in Figure 2. We utilize a pretrained VAE [Rombach *et al.*, 2022] to compress observations into the latent space. Future observations are generated directly within this latent space to leverage the benefits of compressed representations. Finally, the generated latent representations are decoded by the VAE to recover images in pixel space.

Action Embedding. The action input a_τ consists of N relative waypoints (x, y, ϕ) . To ensure continuity, we encode ϕ as $(\cos \phi, \sin \phi)$, forming an $(N, 4)$ vector. This input is projected by a 4-layer MLP into a high-dimensional embedding, which conditions the spatial attention blocks via cross-attention.

Spatial and Temporal Attention. In the 3D U-Net architecture, each processing block comprises three components: CNN module, Spatial Attention module, and Temporal Attention module. Since the computational complexity of the transformer architecture scales quadratically with context

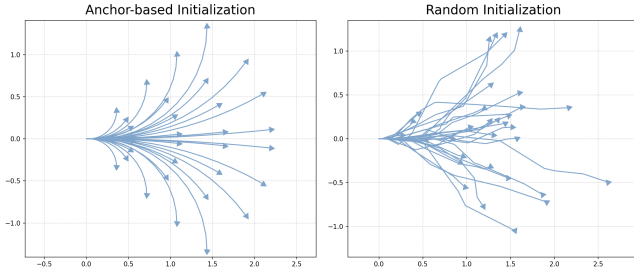


Figure 3: Comparison of anchor-based initialization and random initialization.

length, processing the full spatiotemporal volume globally is computationally prohibitive. We therefore decouple spatial and temporal modeling, as done in prior works [Blattmann *et al.*, 2023; Wang *et al.*, 2023]. The CNN and Spatial Attention modules operate in a frame-wise manner, focusing exclusively on capturing intra-frame spatial dependencies without cross-frame interaction. Conversely, the Temporal Attention module is dedicated to inter-frame information propagation. We employ a window-based attention mechanism [Liu *et al.*, 2021; Gu *et al.*, 2023] for the temporal module. In particular, we partition each frame into $m \times m$ spatial regions (windows). Attention operations are restricted locally, such that a token computes attention scores exclusively with other tokens located within the same spatial window, thereby reducing the context length while maintaining spatiotemporal consistency.

3.3 Training Details

Following the setup described in [Bar *et al.*, 2025], we collect 500 trajectories within a single indoor environment for training. During model training, we adopt a random trajectory sampling strategy: the position of the final frame is selected randomly, and 10 frames are randomly sampled between the current and final frames to generate a single training instance. This approach effectively increases trajectory diversity within the limited dataset.

In our experiments, we observed that relying solely on data collected in the new scene degraded the prediction quality of the navigation world model. To address this, we first train a base model on a large-scale public navigation dataset [Shah *et al.*, 2023a] to obtain a pretrained navigation world model. We then fine-tune this pretrained model using the specific data collected from the new environment. Our results demonstrate that this pretraining strategy significantly enhances navigation performance.

3.4 Navigation with World Model

Leveraging the world model’s ability to predict future observations conditioned on given actions, we implement a model-based planning framework. Specifically, we use the world model to generate future observations for a set of candidate action samples. Each sample is then scored based on its alignment with the specific navigation goal (e.g., image, language or point-goal). We employ the Cross-Entropy Method (CEM) [Rubinstein, 1997] to optimize this process and select the optimal action.

To minimize computational overhead, we limit the sample size to 32 actions at each optimization step. However, we observe that with such a limited sample size, random initialization often fails to sufficiently cover the action space. This results in suboptimal initialization for the planner, ultimately degrading navigation performance. To address this, we employ an anchor-based initialization strategy, where initial candidate trajectories are generated using fixed sets of linear and angular velocities, as shown in Figure 3. Empirical results demonstrate that the performance of such an anchor-based approach significantly outperforms that of random initialization.

4 Generation Experiments

We evaluate the generation quality of the proposed one-step navigation world model in this section.

4.1 Experimental Setup

We collect training datasets from the MP3D dataset [Chang *et al.*, 2017], using the Habitat simulator [Szot *et al.*, 2021]. Each dataset consists of 500 trajectories within the respective indoor scene. All models are trained independently on each of the datasets and tested on unseen trajectories.

We compare the proposed method with the following baselines:

- **NWM** [Bar *et al.*, 2025]. NWM is a navigation world model which employs a Conditional Diffusion Transformer (CDiT) architecture to predict future images autoregressively frame-by-frame. We use its -B variant, due to its comparable parameter scale to our model, and replace its original diffusion model with the shortcut model [Frans *et al.*, 2024], consistent with the approach used in our method.
- **Ours (w/o random traj).** An ablative variant of our method without random trajectory sampling strategy in training.
- **Ours (w/o pretrain).** An ablative variant of our method without first training on large-scale public navigation datasets.

4.2 Generation Performance

We utilize PSNR, SSIM [Wang *et al.*, 2004], LPIPS [Zhang *et al.*, 2018], DreamSim [Fu *et al.*, 2023], and FID [Heusel *et al.*, 2017] to measure the frame-wise similarity between the generated output and ground truth. To evaluate the overall spatiotemporal quality of the generated video, we also introduce FVD [Unterthiner *et al.*, 2018]. Furthermore, given the importance of generation speed, we report the inference time for generating 11 future frames with a batch size of 1 on an NVIDIA H200 GPU. The experimental results are presented in Table 1. Quantitative results demonstrate the superiority of the proposed model. It can be seen that the proposed model surpasses NWM by a wide margin in both per-frame quality and spatiotemporal consistency. Moreover, the proposed model is significantly more computational-efficient, reducing inference time by approximately 45% (0.076s vs.

Method	PSNR \uparrow	SSIM \uparrow	LPIPS \downarrow	DreamSim \downarrow	FID \downarrow	FVD \downarrow	Params (M)	Time (s) \downarrow
NWM	14.557	0.368	0.401	0.336	94.850	27.173	194	0.138
Ours (w/o random traj)	17.196	0.456	0.290	0.286	89.682	18.518	175	0.076
Ours (w/o pretrain)	16.810	0.434	0.300	0.304	98.724	21.720	175	0.076
Ours	17.611	0.473	0.267	0.272	83.826	17.254	175	0.076

Table 1: Generation Results of different methods

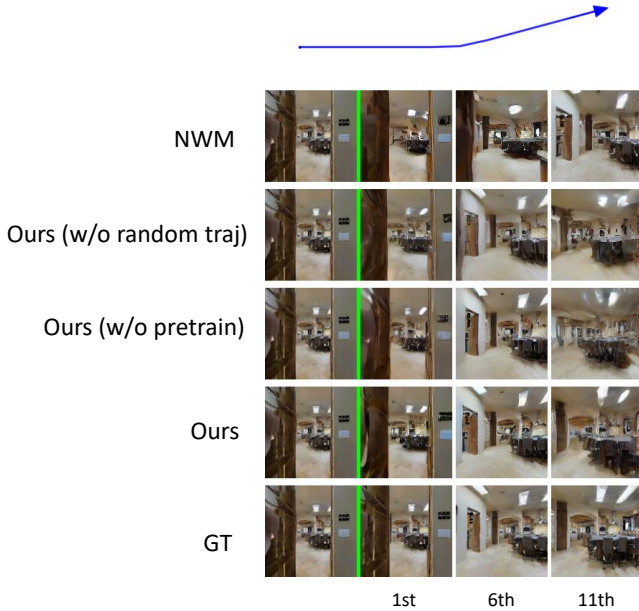


Figure 4: Qualitative comparison of our method against baselines. Given the initial observation, the frames generated by our model achieve higher quality than those of NWM and closely match the ground truth. Furthermore, the visualization demonstrates that random trajectory sampling during training and pretraining on public datasets play a crucial role in performance.

0.138s) with a similar parameter scale. Ablation studies further demonstrate that the random trajectory sampling strategy and pretraining on public datasets notably enhance model generalization.

As illustrated in Figure 4, NWM struggles with precise action execution. The recursive nature of its autoregressive generation leads to compounding errors, resulting in severe position drift from the ground truth. On the other hand, the proposed method mitigates these issues by generating all future frames in a single forward pass. The incorporation of temporal attention allows the model to effectively learn temporal dependencies, ensuring higher fidelity in long-sequence generation. Additionally, the use of random trajectory sampling strategy combined with pretraining on large-scale datasets further improves the visual quality and details of the generated images.

5 Navigation Experiments

5.1 Experimental Setup

Leveraging the proposed world model with task-specific loss functions, our method enables navigation guided by multi-modal goals. We successfully execute image-goal, language-goal and point-goal navigation, significantly outperforming competitive baselines. For CEM optimization used in the proposed method, we use a sample size of 32, select the top 5 samples per iteration, and perform 5 iterations. The experimental evaluation consists of 150 episodes across 5 different scenes for image-goal, language-goal and point-goal navigation. We employ *Success Rate (SR)* and *Success-weighted Path Length (SPL)* to evaluate navigation performance. Additionally, we report the inference time for each method, measured on an NVIDIA H200 GPU.

Apart from the compared methods mentioned in Section 4.1, we also compare the proposed method with several baselines:

- **NoMaD**[Sridhar *et al.*, 2024]. A unified diffusion policy utilizing goal masking to handle both exploration and image-goal navigation.
- **OmniVLA**[Hirose *et al.*, 2025]. An omni-modal robot navigation model built upon the OpenVLA[Kim *et al.*, 2024] backbone.
- **Ours (random init)**. An ablative variant of our method with random initialization in CEM instead of anchor-based initialization, as described in Section 3.4.

To ensure a fair comparison, the NWM baseline is evaluated using the same planning configuration as our method, including the integration of the proposed anchor-based initialization strategy and the use of the same planning loss function.

Image-Goal Navigation. To implement image-goal navigation, we employ LPIPS [Zhang *et al.*, 2018] as loss function to score sampled trajectories. Drawing inspiration from prior vision-based approaches [Shah *et al.*, 2023a; Sridhar *et al.*, 2024], we utilize a topological memory system to achieve long-horizon navigation. Specifically, the process initiates with the first observation. At each time step, a distance estimation network identifies the nearest node in the topological graph to estimate the current location. Subsequently, the image of the adjacent node is fed into the policy system as the immediate target.

Language-Goal Navigation. To implement language-goal navigation, we employ SigLIP [Zhai *et al.*, 2023] as the scoring function to evaluate sampled trajectories. We utilize Qwen2-VL [Wang *et al.*, 2024] to generate navigational

Method	Image-Goal			Language-Goal			Point-Goal		
	SR	SPL	Time (s)	SR	SPL	Time (s)	SR	SPL	Time (s)
NoMaD	16.67	15.13	0.097	-	-	-	-	-	-
OmniVLA	36.67	34.78	0.113	62.67	56.52	0.078	40.00	36.72	0.081
NWM	43.33	38.66	1.086	51.33	45.98	1.613	52.67	47.31	1.688
Ours (w/o random traj)	64.67	61.51	0.765	63.33	56.91	1.179	50.67	45.17	1.290
Ours (w/o pretrain)	64.00	61.11	0.765	65.33	58.19	1.179	48.00	43.79	1.290
Ours (random init)	69.33	62.12	0.765	59.33	50.27	1.179	50.00	43.05	1.290
Ours	72.67	69.10	0.765	69.33	60.90	1.179	50.00	46.24	1.290

Table 2: Navigation results of image-goal, language-goal, and point goal tasks

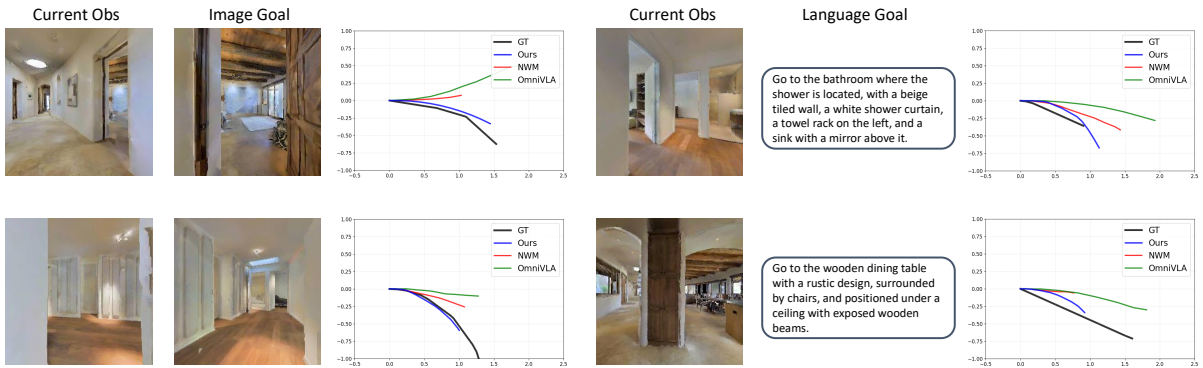


Figure 5: Visualization of trajectories predicted by different methods in image-goal (left) and language-goal (right) navigation.

language instructions conditioned on the target image for the task.

Point-Goal Navigation. To implement point-goal navigation, we incorporate Depth-Anything [Yang *et al.*, 2024] to perform monocular depth estimation on the predicted future images. We formulate a composite planning loss function to evaluate candidate trajectories. Specifically, this loss is defined as the weighted sum of two terms: (1) the Euclidean distance between the terminal point of the sampled trajectory and the target coordinate, and (2) the negative mean depth value in the central region of the predicted image (to penalize proximity to obstacles).

5.2 Navigation Performance Results

The quantitative results in Table 2 demonstrate that the proposed model significantly outperforms both the world-model baseline (NWM) and end-to-end policies (NoMaD, OmniVLA). Specifically, in the image-goal navigation task, our method achieves a Success Rate (SR) of 72.67%, surpassing NWM by a substantial margin of 29.3% and OmniVLA by 36.0%. For language-goal tasks, the proposed approach attains the highest SR of 69.33%, exceeding NWM by 18.0% and OmniVLA by 6.7%. Figure 5 visualizes the trajectories generated by different methods under identical observations. It is evident that world-model-based methods exhibit superior spatial reasoning and semantic understanding capabilities. Specifically, when facing a substantial offset between the current and target difference, end-to-end policies often fail to

capture the underlying spatial relationship, whereas the proposed approach maintains an accurate understanding of the goal-relative geometry. Furthermore, in the point-goal task, our method yields performance comparable to NWM while consistently outperforming OmniVLA, demonstrating the inherent advantages of world-model-based framework. Crucially, compared to NWM, the proposed method exhibits a significant improvement in inference speed. Such a result is attributed to the model’s paradigm to simultaneously predict all future sequence frames, combined with the utilization of computationally efficient spatial-temporal attention.

Loss Function	SR	SPL	Time (s)
BLIP	59.33	51.43	2.183
CLIP	61.33	53.15	1.094
SigLIP (default)	69.33	60.90	1.179

Table 3: Language-goal navigation results of different loss function

5.3 Ablations

Table 2 presents the performance comparison between the proposed full method and two ablation variants. The results underscore the critical roles of both the pretraining and random trajectory sampling strategy employed during training. Furthermore, we evaluate the impact of initialization within the CEM planner by comparing random initialization strategy against the proposed anchor-based initialization strategy. As

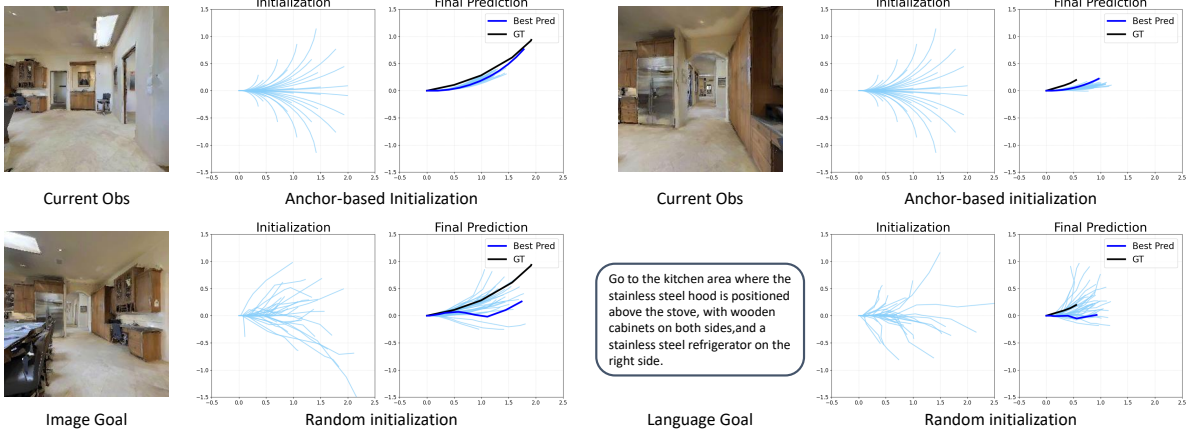


Figure 6: Qualitative comparison of predicted trajectories using anchor-based and random initialization, respectively, in image-goal (left) and language-goal (right) navigation.

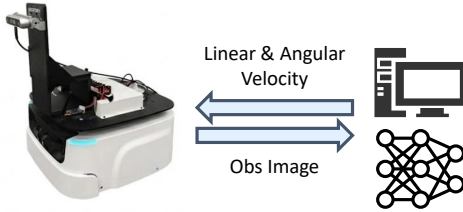


Figure 7: Overview of the robotic platforms in our real-world evaluation.

shown in Table 2, the anchor-based approach is instrumental in boosting navigation performance. This advantage is further corroborated by the qualitative visualization in Figure 6, which reveals that anchor-based initialization yields smoother and more concentrated trajectory samples, thereby facilitating more effective planning.

Furthermore, we observe that the performance of language-goal navigation is highly sensitive to the choice of the planning loss function. To indicate this point, we conduct a comparative analysis using three distinct image-text alignment models—BLIP [Li *et al.*, 2022], CLIP [Radford *et al.*, 2021], and SigLIP [Zhai *et al.*, 2023]—as the guidance objective. The quantitative results are reported in Table 3. It can be found that SigLIP yields the superior navigation performance, outperforming the other image-text alignment models.

6 Real-world Experiments

To further validate the effectiveness of the proposed method, we conduct real-world experiments on a mobile robot platform equipped with an Intel RealSense camera, as depicted in Figure. 7. The system operates via a client-server architecture: the robot transmits real-time observations to a cloud server via a network connection, where the model performs inference and returns control commands (i.e., linear and angular velocities). We conduct 25 trials for each method on each task. The quantitative results, presented in Table 4, in-

Method	Image-Goal	Language-Goal	Point-Goal
NoMaD	40%	-	-
OmniVLA	52%	56%	76%
NWM	48%	32%	68%
Ours	80%	68%	76%

Table 4: Real-world navigation Results

dicate that the proposed approach consistently outperforms baselines in physical environments, demonstrating its robustness and strong generalization capabilities.

7 Conclusion

This work presents a lightweight navigation world model that outperforms end-to-end policies while overcoming the inference speed limitations of traditional world models. Leveraging a one-step generation paradigm and a 3D U-Net backbone with spatial-temporal attention, our approach ensures low latency and robust spatial reasoning. Integrated with an anchor-based initialization planning framework, the proposed system achieves superior results in multi-modal goal navigation across simulation and real-world closed-loop experiments.

Despite these advancements, several limitations remain. First, integrating CEM with the world model necessitates exploration within the whole action space, posing significant challenges for searching complex trajectories. Second, the iterative optimization process requires a trade-off between generation quality and inference speed. In future research, we aim to address these challenges by investigating a navigation world model with a latent action space [Bu *et al.*, 2025] and by constructing a fast-slow dual system [Chen *et al.*, 2025] that combines the predictive power of the world model with a reactive local policy.

References

[Bar *et al.*, 2025] Amir Bar, Gaoyue Zhou, Danny Tran, Trevor Darrell, and Yann LeCun. Navigation world mod-

els. In *Proceedings of the Computer Vision and Pattern Recognition Conference*, pages 15791–15801, 2025.

[Blattmann *et al.*, 2023] Andreas Blattmann, Tim Dockhorn, Sumith Kulal, Daniel Mendelevitch, Maciej Kilian, Dominik Lorenz, Yam Levi, Zion English, Vikram Voleti, Adam Letts, et al. Stable video diffusion: Scaling latent video diffusion models to large datasets. *arXiv preprint arXiv:2311.15127*, 2023.

[Bruce *et al.*, 2024] Jake Bruce, Michael D Dennis, Ashley Edwards, Jack Parker-Holder, Yuge Shi, Edward Hughes, Matthew Lai, Aditi Mavalankar, Richie Steigerwald, Chris Apps, et al. Genie: Generative interactive environments. In *Forty-first International Conference on Machine Learning*, 2024.

[Bu *et al.*, 2025] Qingwen Bu, Yanting Yang, Jisong Cai, Shenyuan Gao, Guanghui Ren, Maoqing Yao, Ping Luo, and Hongyang Li. Univla: Learning to act anywhere with task-centric latent actions. *arXiv preprint arXiv:2505.06111*, 2025.

[Cai *et al.*, 2025] Wenzhe Cai, Jiaqi Peng, Yuqiang Yang, Yujian Zhang, Meng Wei, Hanqing Wang, Yilun Chen, Tai Wang, and Jiangmiao Pang. Navdp: Learning sim-to-real navigation diffusion policy with privileged information guidance. *arXiv preprint arXiv:2505.08712*, 2025.

[Chang *et al.*, 2017] Angel Chang, Angela Dai, Thomas Funkhouser, Maciej Halber, Matthias Niebner, Manolis Savva, Shuran Song, Andy Zeng, and Yinda Zhang. Matterport3d: Learning from rgb-d data in indoor environments. In *2017 International Conference on 3D Vision (3DV)*, pages 667–676. IEEE Computer Society, 2017.

[Chen *et al.*, 2025] Hao Chen, Jiaming Liu, Chenyang Gu, Zhiyuan Liu, Renrui Zhang, Xiaoqi Li, Xiao He, Yandong Guo, Chi-Wing Fu, Shanghang Zhang, et al. Fast-in-slow: A dual-system foundation model unifying fast manipulation within slow reasoning. *arXiv preprint arXiv:2506.01953*, 2025.

[Du *et al.*, 2023] Yilun Du, Sherry Yang, Bo Dai, Hanjun Dai, Ofir Nachum, Josh Tenenbaum, Dale Schuurmans, and Pieter Abbeel. Learning universal policies via text-guided video generation. *Advances in neural information processing systems*, 36:9156–9172, 2023.

[Frans *et al.*, 2024] Kevin Frans, Danijar Hafner, Sergey Levine, and Pieter Abbeel. One step diffusion via shortcut models. *arXiv preprint arXiv:2410.12557*, 2024.

[Fu *et al.*, 2023] Stephanie Fu, Netanel Tamir, Shobhita Sundaram, Lucy Chai, Richard Zhang, Tali Dekel, and Phillip Isola. Dreamsim: Learning new dimensions of human visual similarity using synthetic data. *arXiv preprint arXiv:2306.09344*, 2023.

[Gu *et al.*, 2023] Xianfan Gu, Chuan Wen, Weirui Ye, Jiaming Song, and Yang Gao. Seer: Language instructed video prediction with latent diffusion models. *arXiv preprint arXiv:2303.14897*, 2023.

[Ha and Schmidhuber, 2018] David Ha and Jürgen Schmidhuber. World models. *arXiv preprint arXiv:1803.10122*, 2(3), 2018.

[Hafner *et al.*, 2019] Danijar Hafner, Timothy Lillicrap, Jimmy Ba, and Mohammad Norouzi. Dream to control: Learning behaviors by latent imagination. *arXiv preprint arXiv:1912.01603*, 2019.

[Hafner *et al.*, 2023] Danijar Hafner, Jurgis Pasukonis, Jimmy Ba, and Timothy Lillicrap. Mastering diverse domains through world models. *arXiv preprint arXiv:2301.04104*, 2023.

[Heusel *et al.*, 2017] Martin Heusel, Hubert Ramsauer, Thomas Unterthiner, Bernhard Nessler, and Sepp Hochreiter. Gans trained by a two time-scale update rule converge to a local nash equilibrium. *Advances in neural information processing systems*, 30, 2017.

[Hirose *et al.*, 2024] Noriaki Hirose, Catherine Glossop, Ajay Sridhar, Dhruv Shah, Oier Mees, and Sergey Levine. Lelan: Learning a language-conditioned navigation policy from in-the-wild videos. *arXiv preprint arXiv:2410.03603*, 2024.

[Hirose *et al.*, 2025] Noriaki Hirose, Catherine Glossop, Dhruv Shah, and Sergey Levine. Omnidvla: An omni-modal vision-language-action model for robot navigation. *arXiv preprint arXiv:2509.19480*, 2025.

[Ho *et al.*, 2020] Jonathan Ho, Ajay Jain, and Pieter Abbeel. Denoising diffusion probabilistic models. *Advances in neural information processing systems*, 33:6840–6851, 2020.

[Kim *et al.*, 2024] Moo Jin Kim, Karl Pertsch, Siddharth Karamcheti, Ted Xiao, Ashwin Balakrishna, Suraj Nair, Rafael Rafailov, Ethan Foster, Grace Lam, Pannag Sanketi, et al. Openvla: An open-source vision-language-action model. *arXiv preprint arXiv:2406.09246*, 2024.

[Koh *et al.*, 2021] Jing Yu Koh, Honglak Lee, Yinfei Yang, Jason Baldridge, and Peter Anderson. Pathdreamer: A world model for indoor navigation. In *Proceedings of the IEEE/CVF International Conference on Computer Vision*, pages 14738–14748, 2021.

[LaValle, 2006] Steven M LaValle. *Planning algorithms*. Cambridge university press, 2006.

[Li *et al.*, 2022] Junnan Li, Dongxu Li, Caiming Xiong, and Steven Hoi. Blip: Bootstrapping language-image pre-training for unified vision-language understanding and generation. In *International conference on machine learning*, pages 12888–12900. PMLR, 2022.

[Lipman *et al.*, 2022] Yaron Lipman, Ricky TQ Chen, Heli Ben-Hamu, Maximilian Nickel, and Matt Le. Flow matching for generative modeling. *arXiv preprint arXiv:2210.02747*, 2022.

[Liu *et al.*, 2021] Ze Liu, Yutong Lin, Yue Cao, Han Hu, Yixuan Wei, Zheng Zhang, Stephen Lin, and Baining Guo. Swin transformer: Hierarchical vision transformer using shifted windows. In *Proceedings of the IEEE/CVF international conference on computer vision*, pages 10012–10022, 2021.

[Radford *et al.*, 2021] Alec Radford, Jong Wook Kim, Chris Hallacy, Aditya Ramesh, Gabriel Goh, Sandhini Agarwal, Girish Sastry, Amanda Askell, Pamela Mishkin, Jack Clark, et al. Learning transferable visual models from natural language supervision. In *International Conference on Machine Learning*, pages 8748–8763, 2021.

[Rombach *et al.*, 2022] Robin Rombach, Andreas Blattmann, Dominik Lorenz, Patrick Esser, and Björn Ommer. High-resolution image synthesis with latent diffusion models. In *Proceedings of the IEEE/CVF conference on computer vision and pattern recognition*, pages 10684–10695, 2022.

[Rubinstein, 1997] Reuven Y Rubinstein. Optimization of computer simulation models with rare events. *European Journal of Operational Research*, 99(1):89–112, 1997.

[Shah *et al.*, 2023a] Dhruv Shah, Ajay Sridhar, Arjun Bhorkar, Noriaki Hirose, and Sergey Levine. Gnm: A general navigation model to drive any robot. In *2023 IEEE International Conference on Robotics and Automation (ICRA)*, pages 7226–7233. IEEE, 2023.

[Shah *et al.*, 2023b] Dhruv Shah, Ajay Sridhar, Nitish Dashora, Kyle Stachowicz, Kevin Black, Noriaki Hirose, and Sergey Levine. Vint: A foundation model for visual navigation. In *7th Annual Conference on Robot Learning (CoRL)*, pages 711–733, 2023.

[Shen *et al.*, 2025] Wangtian Shen, Pengfei Gu, Haijian Qin, and Ziyang Meng. Effonav: An effective foundation-model-based visual navigation approach in challenging environment. *IEEE Robotics and Automation Letters*, 2025.

[Song *et al.*, 2020] Jiaming Song, Chenlin Meng, and Stefano Ermon. Denoising diffusion implicit models. *arXiv preprint arXiv:2010.02502*, 2020.

[Sridhar *et al.*, 2024] Ajay Sridhar, Dhruv Shah, Catherine Glossop, and Sergey Levine. Nomad: Goal masked diffusion policies for navigation and exploration. In *2024 IEEE International Conference on Robotics and Automation (ICRA)*, pages 63–70. IEEE, 2024.

[Szot *et al.*, 2021] Andrew Szot, Alexander Clegg, Eric Undersander, Erik Wijmans, Yili Zhao, John Turner, Noah Maestre, Mustafa Mukadam, Devendra Singh Chaplot, Oleksandr Maksymets, et al. Habitat 2.0: Training home assistants to rearrange their habitat. *Advances in neural information processing systems*, 34:251–266, 2021.

[Unterthiner *et al.*, 2018] Thomas Unterthiner, Sjoerd Van Steenkiste, Karol Kurach, Raphael Marinier, Marcin Michalski, and Sylvain Gelly. Towards accurate generative models of video: A new metric & challenges. *arXiv preprint arXiv:1812.01717*, 2018.

[Wang *et al.*, 2004] Zhou Wang, Alan C Bovik, Hamid R Sheikh, and Eero P Simoncelli. Image quality assessment: from error visibility to structural similarity. *IEEE transactions on image processing*, 13(4):600–612, 2004.

[Wang *et al.*, 2023] Jiuniu Wang, Hangjie Yuan, Dayou Chen, Yingya Zhang, Xiang Wang, and Shiwei Zhang. Modelscope text-to-video technical report. *arXiv preprint arXiv:2308.06571*, 2023.

[Wang *et al.*, 2024] Peng Wang, Shuai Bai, Sinan Tan, Shijie Wang, Zhihao Fan, Jinze Bai, Keqin Chen, Xuejing Liu, Jialin Wang, Wenbin Ge, et al. Qwen2-vl: Enhancing vision-language model’s perception of the world at any resolution. *arXiv preprint arXiv:2409.12191*, 2024.

[Yang *et al.*, 2024] Lihe Yang, Bingyi Kang, Zilong Huang, Zhen Zhao, Xiaogang Xu, Jiashi Feng, and Hengshuang Zhao. Depth anything v2. *Advances in Neural Information Processing Systems*, 37:21875–21911, 2024.

[Yang *et al.*, 2025] Yuncong Yang, Jiageng Liu, Zheyuan Zhang, Siyuan Zhou, Reuben Tan, Jianwei Yang, Yilun Du, and Chuang Gan. Mindjourney: Test-time scaling with world models for spatial reasoning. *arXiv preprint arXiv:2507.12508*, 2025.

[Zhai *et al.*, 2023] Xiaohua Zhai, Basil Mustafa, Alexander Kolesnikov, and Lucas Beyer. Sigmoid loss for language image pre-training. In *Proceedings of the IEEE/CVF international conference on computer vision*, pages 11975–11986, 2023.

[Zhang *et al.*, 2018] Richard Zhang, Phillip Isola, Alexei A Efros, Eli Shechtman, and Oliver Wang. The unreasonable effectiveness of deep features as a perceptual metric. In *Proceedings of the IEEE conference on computer vision and pattern recognition*, pages 586–595, 2018.

[Zhang *et al.*, 2025] Zhiwei Zhang, Hui Zhang, Xieyuanli Chen, Kaihong Huang, Chenghao Shi, and Huimin Lu. Latent-space autoregressive world model for efficient and robust image-goal navigation. *arXiv e-prints*, pages arXiv–2511, 2025.

[Zhou *et al.*, 2024] Gaoyue Zhou, Hengkai Pan, Yann LeCun, and Lerrel Pinto. Dino-wm: World models on pre-trained visual features enable zero-shot planning. *arXiv preprint arXiv:2411.04983*, 2024.

[Zhou *et al.*, 2025] Siyuan Zhou, Yilun Du, Yuncong Yang, Lei Han, Peihao Chen, Dit-Yan Yeung, and Chuang Gan. Learning 3d persistent embodied world models. *arXiv preprint arXiv:2505.05495*, 2025.